Progress In Electromagnetics Research Letters, Vol. 107, 39–47, 2022

Miniaturized Antenna Pair for 2.4/5/6 GHz Wi-Fi 6E Operation

Saou-Wen Su* and Peng-Hao Juan

Abstract—The aim of this work is to provide a miniaturized antenna pair, which has a smallest size of 5 mm × 25 mm (about $0.04\lambda \times 0.20\lambda$ at 2.4 GHz) among the recent laptop antennas and yet is capable of 2.4/5/6 GHz Wi-Fi 6E operation with acceptable isolation. The antenna pair comprises two small and symmetrical antenna units. Each unit is identical in geometry and has a coupling strip and a parasitic strip with an in-series inductor. The back-to-back unit arrangement helps better isolation in the 2.4 GHz band. A decoupling coupled strip is introduced between the units with a 5 mm spacing. This floating strip of a half wavelength at about 5.36 GHz attracts the surface currents of one unit excited in the 5/6 GHz bands, which in turn helps much decreased currents entering the port of the other unit. As a result, enhanced isolation can also be achieved in the upper bands.

1. INTRODUCTION

Very recently, the Federal Communications Commission (FCC) approved an additional unlicensed 6 GHz (5925–7125 MHz) band to co-work with the present Wi-Fi 6 (IEEE 802.11ax) operation [1]. With extra 1200 MHz bandwidth, faster wireless speeds and lower-latency services are foreseen. To differentiate wireless devices with this new 6 GHz band from the predecessor, the new terminology dubbed 'Wi-Fi 6E' was created by Wi-Fi Alliance [2]. It should be noted that the Wi-Fi 6E not only includes the 5150–7125 MHz range but also covers the 2.4 GHz (2400–2484 MHz) and 5 GHz (5150–5825 MHz) wireless local area network (WLAN) bands. With this important upgrade, multi-Gbps connections will be available and on a par with fifth-generation (5G) communications [3]. In the laptop industry, this has become a standard specification that the antennas need to operate in the 2.4/5/6 GHz multiple bands to meet Wi-Fi 6E requirements. Some new designs have been presented in [4–6], which also show a low-profile merit for the thin bezel (less than 5 mm [7]) of the laptop display.

To spare space for other electronic components inside the laptop, two antenna units are usually placed in close proximity that is within a quarter wavelength in free space [8]. In this case, small and compact laptop antennas [7, 9–11] are attractive candidates for the units paired in a group for practical applications. This is because the total lateral size can be expected to be small when two same units of these designs are formed with the separation spacing therein. However, high coupling between closely packed antenna units can occur in the same frequency range, which degrades the RF sensitivity in the laptop wireless system.

Adding a decoupling structure as an additional coupled resonator [12–16] is still a very popular decoupling method in the laptop industry. The additional coupling path is incorporated in the near field to counter with the initial antenna port-to-port coupling. These decoupling resonators include the uses of the meandered strip and the T slot in the ground plane [12], the small π-shaped structure [13], the same radiator geometry [14], the loaded strip resonators [15], the multi-branched T-type strip [16], etc. But these studies mainly focus on the design of the decoupling resonators and show large antenna

Received 4 August 2022, Accepted 23 September 2022, Scheduled 19 October 2022
* Corresponding author: Saou-Wen Su (Saou-Wen_Su@asus.com).
The authors are with the Antenna Design Department, Advanced EM & Wireless Communication R&D Center ASUSTek Computer Inc., Taipei 11259, Taiwan.

units with a minimum lateral length larger than 12 mm for WLAN operation. In addition, the total lateral size for two antenna units is also larger than 38 mm. This motivates us to work on miniaturized antenna units that can be paired and decoupled, providing overall smaller design dimensions compared with the previous 2.4/5 GHz laptop antennas.

In this article, we propose a miniaturized antenna pair that not only covers the new 6 GHz band, in addition to the 2.4/5 GHz bands, but may also be the smallest size (5 mm × 25 mm) among the recent laptop antenna-pair designs. The pair has two identical units placed in a symmetric arrangement. Each unit has a coupling strip and a parasitic strip with a chip inductor. The in-series inductor helps reduce the required resonant length for 2.4 GHz operation, in turn obtaining a size reduction. The size of the single unit is 5 mm × 10 mm, smaller than those in [7, 9–11]. Two units are set back-to-back, allowing better isolation in the 2.4 GHz band. A decoupling coupled strip is introduced between the units with a tiny space of 5 mm × 5 mm to enhance the upper-band isolation. Acceptable low port coupling and good radiation performance with low envelop correlation coefficient (ECC) over the 2.4/5/6 GHz bands are also obtained. The proposed prototype was analyzed in simulation and verified by measurement. The design details are described and discussed.

2. MINIATURIZED ANTENNA PAIR AND DESIGN EVOLUTION

Figure 1 illustrates the schematic drawing of the miniaturized antenna pair for the Wi-Fi 6E laptop. The photo of a fabricated prototype is presented in Fig. 2. Two 90 mm mini-coaxial cables were used for antenna feeding through a small gap of 0.5 mm in the experiment. The design is printed on a 0.8-mm dielectric substrate (loss $\tan\delta = 0.02$ and $\varepsilon_r = 4.4$) of size 5 mm × 25 mm and located above a 15-inch 16 : 9 display metal frame of the laptop computer. The pair has two identical antenna units placed in a symmetric arrangement. Each unit comprises a coupling strip and a parasitic strip loaded with a chip inductor between the strip and the antenna ground. In this design, a constant strip width of 0.5 mm is chosen for ease of the studies. The in-series inductor can increase the effective electrical length of the coupled parasitic strip, in turn providing an additional resonant path for lowering antenna frequencies [7].

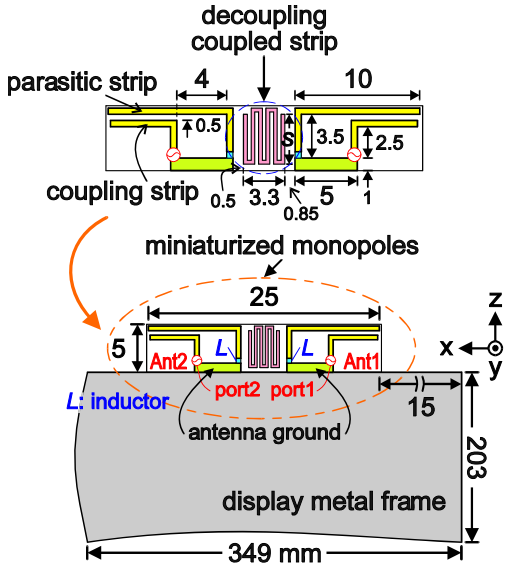

Figure 1. Schematic drawing of the miniaturized antenna pair for Wi-Fi 6E laptops.

The proposed antenna pair evolves from the design of a single antenna unit (Ant1). As seen from the current distribution in the insets of Fig. 3(a), the parasitic and coupling strips produce fundamental resonant modes at 2.45 GHz and 6.14 GHz to cover the 2.4 and 5/6 GHz bands, respectively. The lower-band frequencies can be fine-tuned independently by varying the inductor value L without affecting the impedance bandwidth of the upper bands as shown in Fig. 3(b). In this study, the parasitic-strip length

is 13 mm (about 0.10-λ at 2.4 GHz), corresponding to a 30% size reduction, compared with the case of no chip inductor used. The size of the single unit is 5 mm × 10 mm only, and accordingly, the antenna is ideal to be paired with the same for multiple-input multiple-output (MIMO) antenna applications.

Further, two units (Ant1, Ant2) are set back-to-back with their parasitic strips facing each other and separated by a 5 mm spacing. This arrangement allows better isolation in the 2.4 GHz band, compared with the duplicated unit (Ant2) in the same direction [compare Figs. 4(a) and 4(b)]. The lower-band isolation can be improved by 5 dB (from 8 to 13 dB). It is noteworthy that the isolation is still better than 10 dB even if the separation distance is 1 mm (not shown for brevity). That is, the design of the back-to-back unit set-up is inherently decoupled in the 2.4 GHz band. However, the coupling over the 5 and 6 GHz bands is still high, and the isolation less than 10 dB is also unacceptable in the laptop industry.

To enhance the upper-band isolation, a decoupling coupled strip meandering in symmetrical structure is inserted within the tiny realty space of 5 mm × 5 mm. The strip width is 0.3 mm and

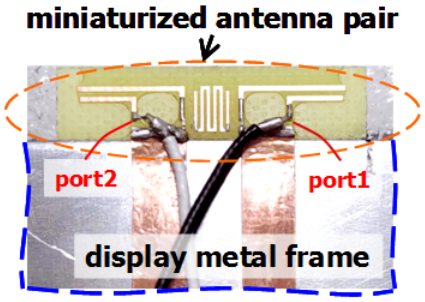

Figure 2. Photo of a fabricated prototype.

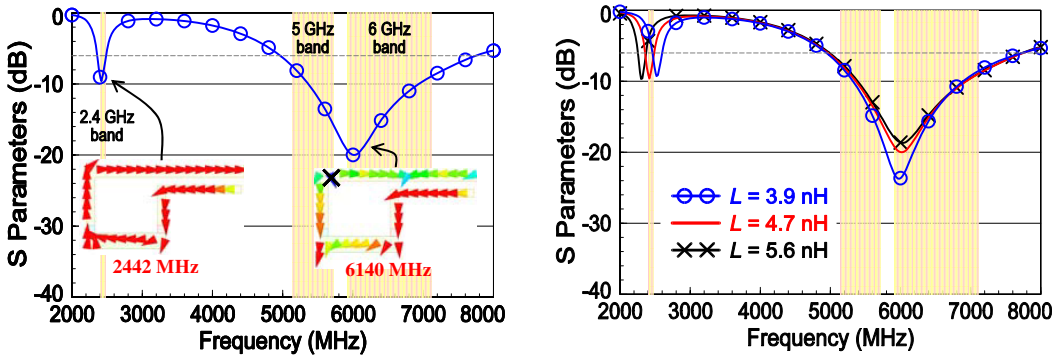

Figure 3. (a) Reflection coefficients of a single antenna unit (Ant1); the inductor $L = 4.7$ nH. (b) Reflection coefficients as a function of the decoupling inductor L.

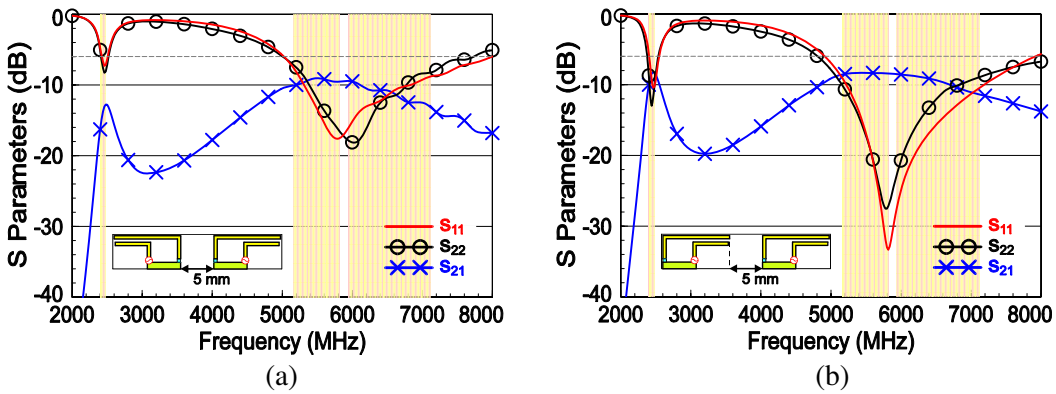

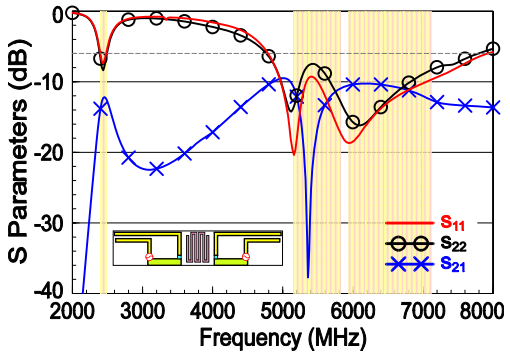

Figure 4. S parameters (S_{11}, S_{22} for Ant1 and Ant2, S_{21} between antenna units). Two units separated by a 5 mm spacing and arranged, (a) back-to-back and (b) in the same direction, (c) proposed design.

has an averaged resonant length of 27.5 mm. As shown in Fig. 4(c) for the proposed design, a large dip in the transmission coefficient (S_{21}) curve at about 5.36 GHz can be easily observed. The isolation is improved by 29 dB (from 9 to 38 dB) and by more than 10 dB over the entire 5150–7125 MHz range. It is mainly because this 'floating' strip resonator strongly coupled with Ant1 when Ant1 is excited can directly attract more upper-band surface currents, not via the ground plane, such that much decreased currents (less magnitude) enter the Ant2 port. As a result, enhanced isolation over the 5 and 6 GHz bands can be achieved.

Figure 5 shows the S parameters as a function of the length (s) of the decoupling coupled strip. It can first be seen that the length of the strip does not affect the 2.4 GHz band but rather the 5 GHz band (5150–5825 MHz). The longer the strip length is, the lower antenna frequencies the frequency dip in the transmission coefficient (S_{21}) shifts toward. Secondly, because there exists a hump (less matched impedance) in the reflection coefficient, both the impedance bandwidth and smaller S_{21} need to be met when choosing the strip length (s). In fact, the decoupling coupled strip is a half wavelength resonator at the frequency dip of S_{21}, and in this case, the 4 mm length (s) corresponds to a total strip length of about half wavelength at 5.36 GHz. The preferred parameters studied here were all obtained with the aid of Ansys HFSS an electromagnetic solver [17].

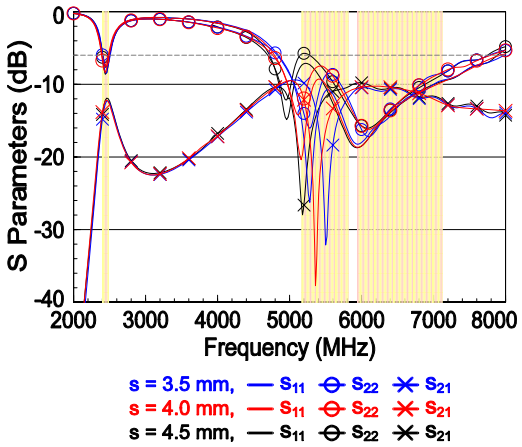

Figure 5. S parameters as a function of the length (s) of the decoupling coupled strip.

3. RESULTS AND DISCUSSIONS

Figure 6(a) shows the simulated and measured reflection and transmission coefficients for the proposed antenna pair. The experimental results agree with the simulation. The difference can be caused by

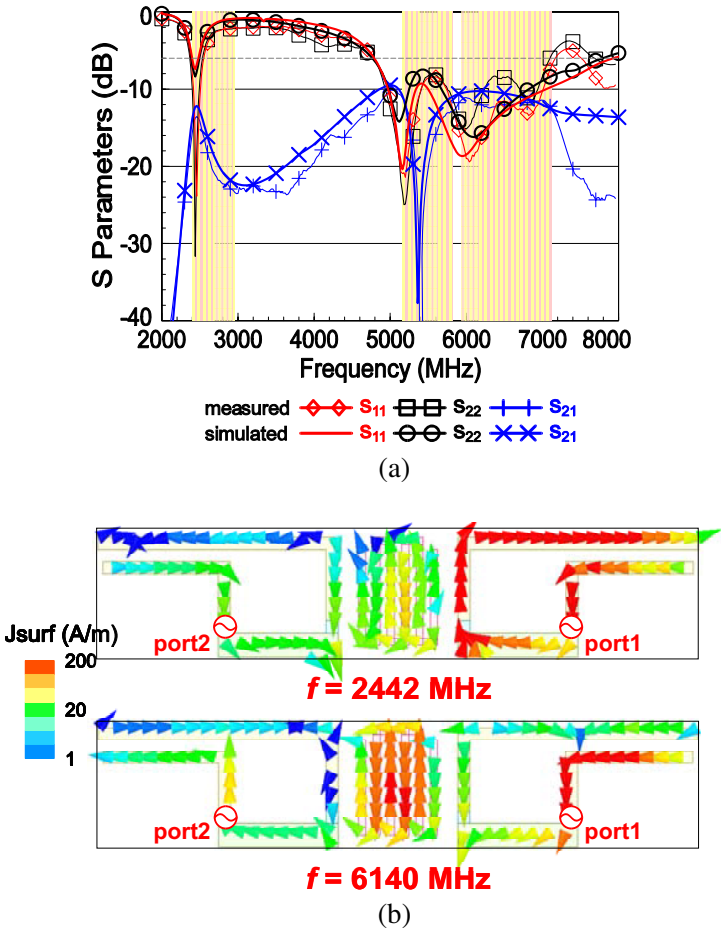

Figure 6. (a) Simulated and measured S parameters; $L = 4.7\,\text{nH}$, $s = 4\,\text{mm}$. (b) Surface current distribution of Ant1 excited at 2442 and 6140 MHz.

the inductor fabrication tolerance and the use of the coaxial cables in the measurement. The inductor used in this paper is of the wire wound type from Murata LQW series, which has higher quality factor (Q) and is also recommended for antenna matching. For the two antenna units, the $-6\,\text{dB}$ impedance bandwidth from the reflection coefficient (S_{11} for Ant1, S_{22} for Ant2) both cover the frequency bands of interest for 2.4 5/6 GHz operation. Note that the $-6\,\text{dB}$ impedance is also acceptable to industrial laptop antenna designs. The measured transmission coefficients (S_{21}) are lower than -14 and $-11\,\text{dB}$ in the 2.4 and 5/6 GHz bands, respectively. The dip seen in the measured S_{21} curve is about $-51\,\text{dB}$ at 5.4 GHz.

Figure 6(b) presents the current distribution of Ant1 excited at 2442 and 6140 MHz. The magnitude in the color bar is set the same for both lower- and upper-band excitation. First, most of the strong surface currents at 2442 MHz are seen populated on Ant1 unit, while relatively weak currents are found on the decoupling coupled strip and the other unit, Ant2. This phenomenon can be expected. Because as previously discussed, the lower-band operation is inherently decoupled, and the said decoupling strip is not designed for decoupling the 2.4 GHz band. Second, for the upper-band excitation at 6140 MHz, high-intensity currents are distributed on the Ant1 coupling strip and the decoupling strip resonator. This is quite straightforward because the coupling strip mainly contributes to the 5/6 GHz bands as seen in the current inset of Fig. 3(a). Also, the results indicate that this floating strip can attract more coupled currents from the antenna unit (Ant1) excited in the upper band, which in turn helps decrease the currents entering the port of the other unit (Ant2) to achieve enhanced isolation.

The reactive near-field radiation patterns for Ant1 excited at 5.36 GHz for the proposed and reference designs are presented in Fig. 7. The radius with port1 as the center for observing the field in

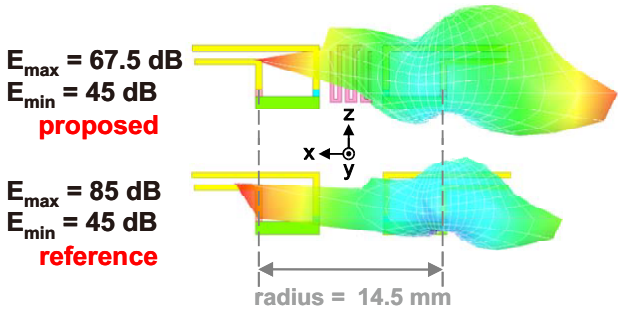

Figure 7. Reactive near-field radiation patterns at 5.36 GHz for the proposed and reference designs with the radius of 14.5 mm (port-to-port distance).

the simulation was set to 14.5 mm. This length is the same as the port1-to-port2 distance, which has the effective range that the reactive near field of the excited unit (Ant1) affects its counterpart unit (Ant2). In this case, the reference shows the large field intensity, covering port2 and the coupling strip of Ant2. For the proposed design, the maximum field strength is not in the direction of port2. In fact, two peaks aiming at the corner of the Ant2 coupling strip and the open ends of Ant1 (opposite direction of Ant2) can be observed. These properties suggest that the large currents on the decoupling strip can attract the reactive near field in the case of the port-to-port radius and redirect the fields away from the receiving unit.

The radiation performance was tested at our MVG SG 24 laboratory, which utilizes the multi-probe array and can measure the spectrum up to 10 GHz [18]. Figs. 8(a), 8(b), 8(c), 8(d) plot the simulated and measured 2-D radiation patterns. The E-total fields at the central frequencies at 2442 and 6140 MHz respectively for the 2.4 and 5/6 GHz bands are presented. Because of both polarization coexistence in the real multipath environment, our empirical studies on actual laptops show that the E-total gain patterns (instead of separate E_θ and E_φ fields) can decide the final data throughput performance. In the 2.4 GHz band, the omnidirectional patterns can be easily found in the x-y plane. The quasi-omnidirectional patterns in the x-z and y-z planes for Ant2 are also obtained in Fig. 8(c). As for 5/6 GHz operation, the radiation ripples are observed in three principal planes with more radiation diverted to the $+z$ direction above the display metal frame.

The peak antenna gain and antenna efficiency were measured, and the cable and antenna mismatch losses in the experiment were taken into account. Related results are shown in Fig. 9. Note that the measured antenna efficiency was obtained by summing the total antenna radiated power over 3-D spherical radiation and dividing it by the 0 dBm given power. For Ant1 over the 2.4 and 5/6 GHz bands, the peak antenna gain is about 1.7–2.0 and 4.0–5.9 dBi with antenna efficiency greater than 40% and 63% respectively. As for Ant2, the gain is in the range of 1.7–2.0 and 4.3–5.7 dBi with antenna efficiency greater than 42% and 65% in the lower and upper bands. The low antenna efficiency for Ant1 and Ant2 are largely owing to the loss of the in-series inductor embedded between the parasitic strip and the antenna ground. Nevertheless, the antenna efficiency around 40% is still acceptable to the industrial laptop-antenna designs.

Figure 10 shows the measured envelope correlation coefficients (ECC) between two antenna units. This figure of merit is derived from the calculations of the two complex far fields [19] in the uniform multipath surroundings [20] and reflects the similarity between the radiation characteristics of the antennas. In this work, low ECC smaller than 0.46 and 0.06, respectively, are obtained over the 2.4 and 5/6 GHz bands. For mobile devices, the ECC smaller than 0.5 [21, 22] is considered a low value for good antenna diversity gain.

A comparison table, Table 1, for this work and other cited WLAN antennas is provided in this section. Several critical aspects are tabulated, including the designed frequency bands, antenna size and spacing, isolation, antenna gain and efficiency. For fair comparison, the electrical length in free-space wavelength λ at the lowest designed frequency is used for antenna size and spacing. In addition, the isolation is a positive value (negative value of transmission coefficient). As far as the authors are concerned, the proposed design has the smallest footprint and yet covers more bands (2.4/5/6 GHz) among WLAN notebook antennas in Table 1.

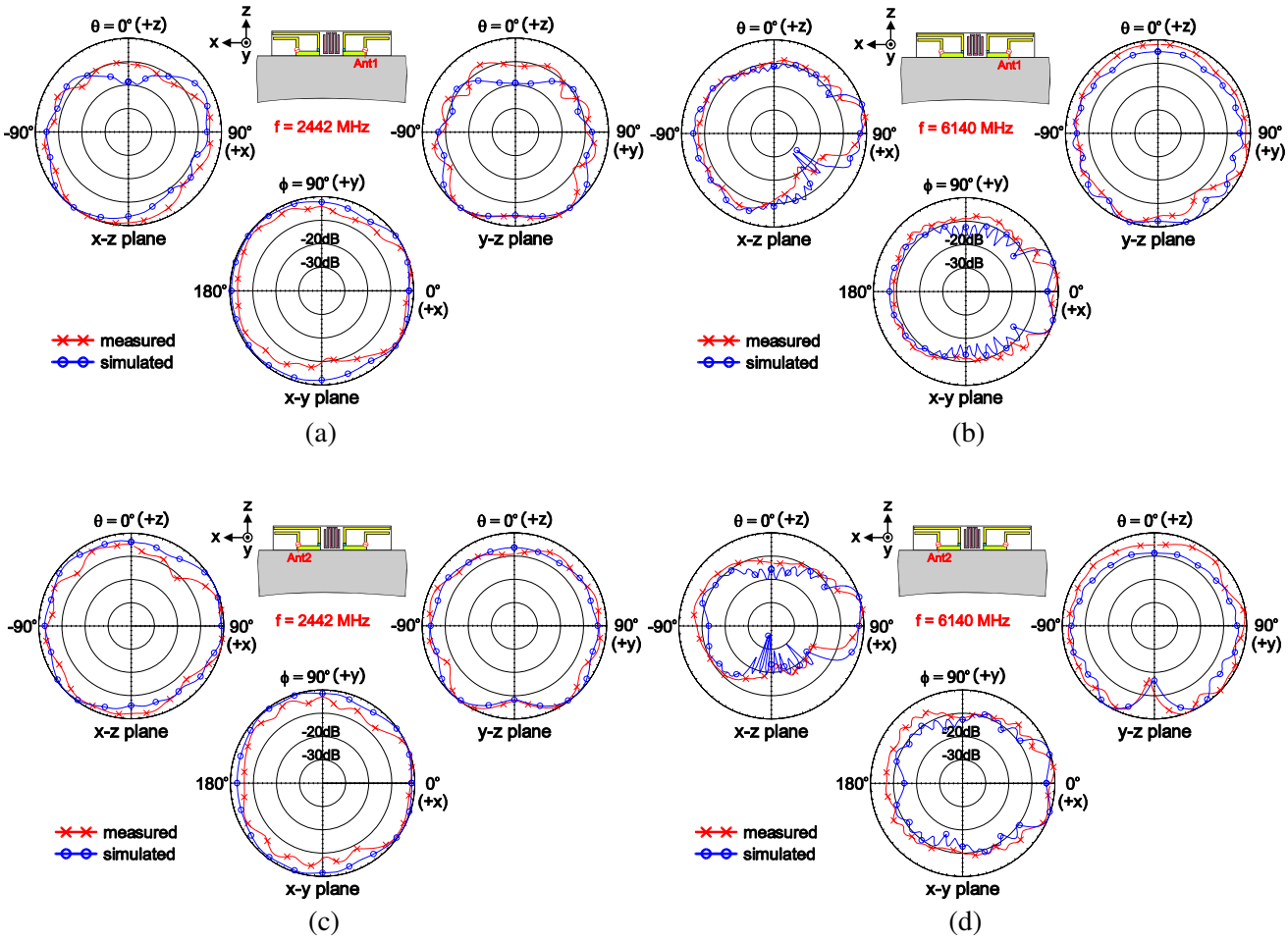

Figure 8. Simulated and measured 2-D radiation patterns (E-total) at 2442 and 6140 MHz. (a) and (b) for Ant1. (c) and (d) for Ant2.

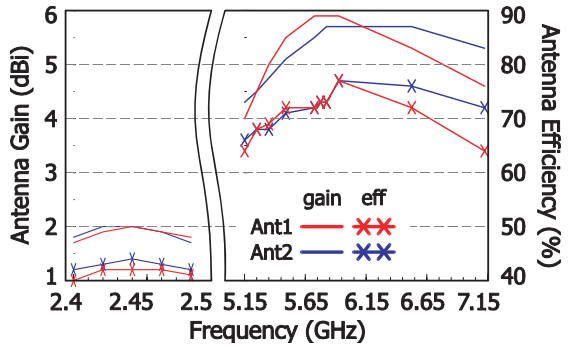

Figure 9. Measured antenna gain and antenna efficiency for Ant1 and Ant2.

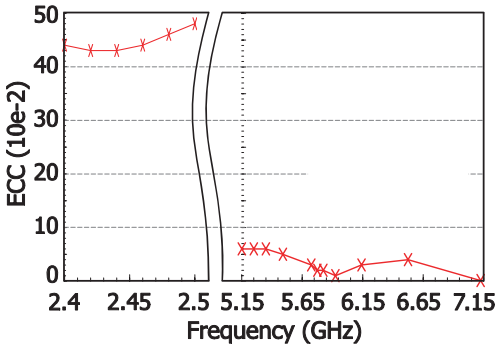

Figure 10. Measured ECC calculated from the radiation patterns of Ant1 and Ant2.

Table 1. Comparison of the proposed work and other cited WLAN antennas [12–16]. λ is the free-space wavelength at the lowest designed frequency. Isolation is shown as the largest value over all the bands.

Ref.	Bands (GHz)	Size (λ)	Spacing (mm)	Isolation (dB)	Gain (dBi) in Lower/Upper Bands	Eff. (%)* in Lower/Upper Bands
[12]	2.4/5 (−10 dB)	0.06×0.37	14.4 (0.11-λ)	15	N.A.	76/59 (Ant1&2)
[13]	2.4/5 (−9.5 dB)	0.04×0.30	2 (0.016-λ)	16	3.6–4.8/3.4–4.5 (Ant1) 2.3–4.2/3.6–4.6 (Ant2)	52/67 (Ant1) 49/64 (Ant2)
[14]	2.4/5 (−9.5 dB)	0.04×0.32	1.6 (0.013-λ)	15	1.4–1.7/3.2–4.6 (Ant1) 1.3–1.8/3.9–5.3 (Ant2)	32/60 (Ant1) 34/57 (Ant2)
[15]	2.4/5 (−9.5 dB)	0.04×0.32	4 (0.032-λ)	17	2.3/3.8-4.7 (Ant1) 2.9/4.2-5.1 (Ant2)	43/64 (Ant1) 44/63 (Ant2)
[16]	2.4/5 (−10 dB)	$0.03 \times 0.05 \times 0.4$	20 (0.16-λ)	15	N.A.	N.A.
Proposed	2.4/5/6 (−6 dB)	0.04×0.2	5 (0.04-λ)	11	1.7–2.0/4.0–5.9 (Ant1) 1.7–2.0/4.3–5.7 (Ant2)	40/60 (Ant1) 42/65 (Ant2)

N.A.: Not Available

*Eff.: Efficiency (%) is shown as the minimum percentage (%) in the band(s).

4. CONCLUSION

A printed, miniaturized, two-unit antenna design, covering the 2.4/5 GHz and the new 6 GHz bands with an extremely small footprint, for integration into laptops has been introduced. The footprint of 5 mm × 25 mm may be the smallest pair of laptop antennas in recent works. The coupling strip of the antenna unit produces a wideband to cover the 5150–7125 MHz range. The parasitic strip embedded with the chip inductor can achieve a size reduction for operating in the 2.4 GHz band. The two antenna units are set back to back to obtain better isolation larger than 14 dB in the 2.4 GHz band, and the decoupling coupled strip is inserted between the units for isolation enhancement (S_{21} dip from −9 to −38 dB) over the 5 and 6 GHz bands. The measured efficiency in the 2.4 and 5/6 GHz bands exceeds 40% and 63% for Ant1 and 42% and 65% for Ant2. The low efficiency in the 2.4 GHz band is owing to the loss of the in-series inductor. Overall, this work can be valuable in industrial, laptop antenna designs that require small-sized and yet decoupled Wi-Fi 6E antennas.

REFERENCES

1. Federal Communications Commission, "FCC opens 6 GHz band to Wi-Fi and other unlicensed uses," https://www.fcc.gov/document/fcc-opens-6-ghz-band-wi-fi-and-other-unlicensed-uses-0.

2. Wi-Fi Alliance, "Wi-Fi Alliance brings Wi-Fi 6 into 6 GHz," https://www.wi-fi.org/news-events/newsroom/wi-fi-alliance-brings-wi-fi-6-into-6-ghz.
3. Wireless Broadband Alliance, "WBA's first phase of Wi-Fi 6E trials shows the massive potential of Wi-Fi in the 6 GHz band," https://www.realwire.com/releases/WBAs-First-Phase-of-Wi-Fi-6E-Trials-Shows-the-Massive-Potential-of-Wi-Fi.
4. Su, S. W. and C. C. Wan, "Asymmetrical, self-isolated laptop antenna in the 2.4/5/6 GHz Wi-Fi 6E bands," *Proc. Int. Symposium on Antennas and Propagat.*, 1–2, Taipei, Taiwan, 2021.
5. Su, S. W., D. P. Yusuf, and F. H. Chu, "Conjoined, Wi-Fi 6E MIMO antennas for laptops," *Proc. Int. Symposium on Antennas and Propagat.*, 1–2, Taipei, Taiwan, 2021.
6. Su, S. W., "Compact, small, chip-inductor-loaded Wi-Fi 6E monopole antenna," *IEEE Int. Symposium on Antennas and Propagat.*, 1–2, Singapore, 2021.
7. Su, S. W., C. T. Lee, and S. C. Chen, "Compact, printed, tri-band loop antenna with capacitively-driven feed and end-loaded inductor for notebook computers," *IEEE Access*, Vol. 6, 6692–6699, 2018.
8. Mak, A. C. K., C. R. Rowell, and R. D. Murch, "Isolation enhancement between two closely packed antennas," *IEEE Trans. Antennas Propagat.*, Vol. 56, 3411–3419, 2008.
9. Su, S. W., "Very-low-profile, 2.4/5-GHz WLAN monopole antenna for large screen-to-body-ratio notebook computers," *Microw. Opt. Technol. Lett.*, Vol. 60, 1313–1318, 2018.
10. Su, S. W., "Capacitor-inductor-loaded, small-sized loop antenna for WLAN notebook computers," *Progress In Electromagnetics Research M*, Vol. 71, 179–188, 2018.
11. Su, S. W., "Very-low-profile, small-sized, printed monopole antenna for WLAN notebook computer applications," *Progress In Electromagnetics Research Letters*, Vol. 82, 51–57, 2019.
12. Deng, J. Y., J. Y. Li, L. Zhao, and L. X. Guo, "A dual-band inverted-F MIMO antenna with enhanced isolation for WLAN applications," *IEEE Antennas Wireless Propagat. Lett.*, Vol. 16, 2270–2273, 2017.
13. Su, S. W., C. T. Lee, and Y. W. Hsiao, "Compact two-inverted-F-antenna system with highly integrated π-shaped decoupling structure," *IEEE Trans. Antennas Propagat.*, Vol. 67, 6182–6186, 2019.
14. Su, S. W. and Y. W. Hsiao, "Small-sized, decoupled two-monopole antenna system using the same monopole as decoupling structure," *Microw. Opt. Technol. Lett.*, Vol. 61, 2049–2055, 2019.
15. Chang, W. H. and S. W. Su, "Very-low-profile, decoupled, hybrid, two-antenna system using top-loaded, coupled strip resonator for notebook computer applications," *Progress In Electromagnetics Research M*, Vol. 84, 63–72, 2019.
16. Chen, Y.-R. and W.-S. Chen, "Design of MIMO WLAN 2.4/5.2/5.8 and 5G sub-6 GHz antennas for laptop computer applications," *IEEE Int. Workshop on Electromagnetics*, 1–2, Penghu, Taiwan, 2020.
17. Ansys HFSS, Ansys Inc., http://www.ansys.com/Products/Electronics/ANSYS- HFSS.
18. SG 24-S, MVG, https://www.mvg-world.com/en/products/antenna-measurement/multi-probe-systems/sg-24.
19. Blanch, S., J. Romeu, and I. Corbella, "Exact representation of antenna system diversity performance from input parameter description," *Electronics Lett.*, Vol. 39, 705–707, 2003.
20. Sharawi, M. S., "Printed multi-band MIMO antenna systems and their performance metrics," *IEEE Antennas and Propagat. Mag.*, Vol. 55, 218–232, 2013.
21. Vaughan, R. G. and J. B. Andersen, "Antenna diversity in mobile communications," *IEEE Trans. Vehicular Technol.*, Vol. 36, 149–172, 1987.
22. Jha, K. R. and S. K. Sharma, "Combination of MIMO antennas for handheld devices," *IEEE Antennas and Propagat. Mag.*, Vol. 60, 118–131, 2018.